Hypothesis

MOLECULAR TUNNELLING IN CARBON MONOXIDE BINDING TO HEMOGLOBIN

Joshua JORTNER and Jens ULSTRUP+

Department of Chemistry, Tel-Aviv University, Tel-Aviv, Israel and +*Chemistry Department A, Building 207, The Technical University of Denmark, 2800 Lyngby, Denmark*

Received 1 December 1978

1. Introduction

Electron transfer (ET) [1–4] and atom or molecular group transfer (AT) [5–9] reactions constitute the most important elementary steps in a variety of biological processes. During the last decade the dynamics of several elementary biological processes were investigated over a broad temperature range from about 2 K up to room temperature. Notable examples are the light-induced oxidation of cytochrome *c* by optically excited bacteriochlorophyll [1–3], the recombination of CO and hemoglobin [9], and the production of prelumirhodopsin from electronically-excited rhodopsin [7]. In all three cases the unimolecular rate was found to be finite and nearly temperature independent at low temperatures, manifesting the effects of nuclear tunnelling, while with increasing temperature the rate changes within a narrow temperature interval into an activated rate exhibiting Arrhenius-type temperature dependence. In a microscopic theory for ET and AT processes two classes of reactions must be distinguished:

(1) Adiabatic processes which proceed on a single potential energy surface. Most AT reactions probably belong to this category.
(2) Nonadiabatic processes involving a transition between two potential energy surfaces which correspond to two (weakly-coupled) distinct zero-order electronic configurations.

The theory of ET in biological systems as nonadiabatic multiphonon processes is now well developed [10–14] being isomorphous with the general quantum mechanical theory of homogeneous and heterogeneous ET processes [15–17]. On the other hand, the theoretical framework for AT processes [16,18,19] is far less comprehensive. In this note we advance a theory of nonadiabatic AT reactions in biological systems, with a specific application to the low-temperature recombination of CO with hemoglobin (hb) [9].

2. The CO/hb recombination reaction

The recombination of CO with β-subunits of hb and derivatives of this compound has been studied over the temperature interval 2–300 K [9]. At high temperatures CO escapes into the outer solvent and passes several barriers on its way back to its coordination site. At temperatures below 180 K the system has only to overcome a single barrier. At these low temperatures the 'pocket' which surrounds the heme group is sealed off thus trapping the CO molecule. The experimental data furthermore showed [9]:

(1) The rebinding kinetics does not exhibit exponential decay but follows a power law. This effect originates from the freezing of different conformational states at the low temperatures.
(2) The average rates (or rather $\tau_{0.75}^{-1}$ where $\tau_{0.75}$ refers to the time when the deoxy-hb concentration has dropped to 75% of its initial value) are practically temperature independent in the range 2–10 K.
(3) The transition from the tunnelling range (2–10 K) to the temperature-activated range occurs in the region 10–20 K. Above this region $\tau_{0.75}^{-1}$ is temperature dependent corresponding to an apparent activation energy of E_A = 0.045 eV.

Consider the nuclear configurational changes

accompanying the CO/hb recombination. Initially the heme Fe atom is located out of the heme plane. Crystallographic data are still incomplete. Values of 0.3 Å, 0.55 Å, and 0.75 Å have been reported [20–24] for the displacement of the Fe atom. The heme group is also linked to the protein residue at its peripheri via axial coordination of a 'proximal' histidine to a fifth coordination site of Fe, while the sixth site is vacant. In the bound CO–hb state the Fe atom is shifted into the heme plane [25], while the CO molecule is now bound to the Fe atom. Recent structural data show that for related model compounds the Fe–C–O unit is linear [26]. Next, we consider the change in the electronic states involved. The CO-free five-coordinated heme group is in the high-spin electronic state ($S = 2$), while the heme group is in the low-spin state ($S = 0$) in the bound CO–hb and CO–mb complexes [25].

3. Nonadiabatic AT theory

Our theory of nonadiabatic multiphonon AT processes is formulated as follows:

(1) The entire electronic–nuclear system can be adequately characterized by two distinct zero-order electronic configurations, corresponding to the high-spin ($S = 2$) and the low-spin ($S = 0$) states.

(2) For each electronic state we can construct a many-dimensional (Born-Oppenheimer) potential energy surface determined by the nuclear displacements of the entire system. A set of vibrational levels for both the initial and final state nuclear potential energy surfaces can subsequently be found.

(3) A microscopic rate constant is derived by considering the system to be initially present in a vibrational level of the initial potential energy surface. Residual second-order spin–orbit interactions which were not incorporated in the Hamiltonian of the zero-order pure spin states couple each initial vibronic level to a manifold of vibronic levels which belong to the final potential surface, and which are degenerate with the initial state level.

(4) Provided that the residual spin–orbit coupling which induces the process is weak relative to the characteristic vibrational frequencies, all the microscopic rate processes can be described in terms of time-dependent perturbation theory. This is the basic feature of the non-adiabatic description of the rate process.

(5) The time-dependent perturbation theory results in microscopic rate constants determined by the Franck-Condon overlap integrals of the nuclear wave functions which can be handled by the theory of multiphonon processes [15–17, 27–29].

(6) The macroscopic nonadiabatic rate is finally expressed as a thermal average of the microscopic rates, the Gibbs averaging being taken over the manifold of initial vibrational levels.

The nonadiabatic AT process is thus essentially viewed as a nonradiative multiphonon process analogous to a variety of other nonadiabatic processes in solid-state physics, molecular physics, and solution chemistry including nonadiabatic ET.

Following the procedure generally applied in the theory of nonradiative processes in a dense medium the thermally-averaged rate constant, W, can be expressed in the form:

$$W = \frac{2\pi}{\hbar} |V_{ab}|^2 Z^{-1} \sum_{v} \sum_{w} \exp(-E^{\circ}_{av}/k_B T) \, |(\chi^{\circ}_{av}/\chi^{\circ}_{bw})|^2 \delta (E^{\circ}_{av} - E^{\circ}_{bw})$$

$$Z = \sum_{v} \exp(-E^{\circ}_{av}/kT) \qquad (1)$$

where χ°_{av} and χ°_{bw} are the nuclear wave functions in the initial (a) and final (b) electronic state, v and w are the nuclear quantum numbers in these two states, E°_{av} and E°_{bw} are the corresponding energies, Z is the partition function for the nuclear motion, V_{ab} is the electronic spin–orbit coupling matrix element which couples the initial and final states, ΔE is the energy gap, i.e., the difference between the energies of the minima of the initial and final state potential energy surface, k_B is the Boltzmann constant, and T is the absolute temperature. The macroscopic nonadiabatic rate constant is expressed as a product of the electronic coupling term and a thermally-averaged Franck-Condon vibrational overlap integral. The delta functions insure the conservation of the total energy.

4. Model calculations for the CO/hb system

The electronic coupling combines zero-order pure spin states of total spin quantum numbers, S=2 and S=0. This shows:

(1) That spin–orbit coupling must be involved;

(2) Since the spin–orbit coupling is a one-electron operator obeying the selection rule $\Delta S = \pm 1$, the coupling matrix element must therefore be a second-order term of the form:

$$V_{ab} \simeq \langle H_{SO} \rangle_{ac} \langle H_{so} \rangle_{cb} / \Delta\epsilon \qquad (2)$$

where $\langle H_{SO} \rangle$ is the spin–orbit coupling integral with respect to the initial, final, and intermediate (c) states and $\Delta\epsilon$ the energy gap between the state c and either the state a or b. Inserting typical values of $\langle H_{SO} \rangle_{ac}$ and $\langle H_{SO} \rangle_{cb}$ of 100 cm^{-1} and $\Delta\epsilon \simeq 1$ eV gives a crude estimate of $V_{ab} \simeq 1$ cm^{-1}.

Three 'intramolecular' coordinates undergo a large equilibrium shift during the reaction and are therefore expected to contribute to the Franck-Condon nuclear overlap integrals in eq. (1).

(1) The motion of the Fe atom which can be viewed as a metal–ligand bending mode coupled to deformational modes in the heme plane. The corresponding frequencies are unknown, but values in the region 100–200 cm^{-1} have been obtained for simple heme complexes [30] and from model calculations [31]. Moreover, the equilibrium configuration of this mode is shifted by 0.3–0.5 Å during the process.

(2) CO is initially weakly associated with the 'distal' histidine, while it is bound to Fe in the final state. Since the configurational changes associated with this mode are unknown, we shall ignore its contribution to eq. (1). This approximation is likely to be adequate in view of the presumably much larger frequency (and large equilibrium coordinate displacement) of the Fe–heme mode, but can otherwise be relaxed if warranted by structural and spectroscopic data.

(3) The relative motion of the heavy Fe–heme and CO–histidine groups is characterized by very low frequencies due to the large reduced mass (which includes part of the protein structure) associated with this motion. This low-frequency motion is not likely to exhibit a large configurational change and it is reasonably incorporated with the medium modes. We shall thus identify $\chi^{\circ}_{a\nu}$ and χ°_{bw} in eq. (1) solely with the Fe motion relative to the heme plane.

By adopting the harmonic approximation for this nuclear motion we can exploit a vast literature on multiphonon processes in other fields to evaluate the Franck-Condon factors. Thus, if the Fe–heme mode is characterized by harmonic potentials of frequency ω in both states, then the nuclear configurational change is specified by the reduced displacement $\Delta = d(\mu\omega/\hbar)^{1/2}$ where d is the coordinate distance between the minima of the two potential surfaces (the shift distance of the Fe atom) and μ the mass associated with the motion. The coupling strength of this mode is then $S = \Delta^2/2$, and the vibrational reorganization energy $E_r = S\hbar\omega$. The temperature dependence is reflected in the thermally-averaged (Bose) occupation number $\bar{\nu} = [\exp(\hbar\omega/k_BT) - 1]^{-1}$. The single-mode rate constant [11] assumes the form:

$$W = \frac{2\pi}{\hbar^2\omega} |V_{ab}|^2 \exp[-S(2\bar{\nu}+1)] I_p \{2S[\bar{\nu}(\bar{\nu}+1)]^{1/2}\} [(\bar{\nu}+1)/\bar{\nu}]^{p/2} \qquad (3)$$

where $p = |\Delta E|/\hbar\omega$ is the normalized energy gap, and I_p the modified Bessel function of order p. Equation (3) exhibits a continuous transition from a low-temperature tunnelling expression ($2S[\bar{\nu}(\bar{\nu}+1)]^{1/2} \ll 1$, or $\hbar\omega \gg k_BT$):

$$W = (2\pi |V_{ab}|^2/\hbar^2\omega) \exp(-S) S^p/p! \qquad (4)$$

to a high-temperature activated rate expression ($2S[\nu(\nu+1)]^{1/2} \gg 1$, or $\hbar\omega \ll k_BT$):

$$W = (\pi/k_BT S\hbar^2\omega)^{1/2} |V_{ab}|^2 \exp[-(\Delta E + S\hbar\omega)^2/4S\hbar\omega k_BT] \qquad (5)$$

with a Gaussian-type activation energy $E_A = (\Delta E + S\hbar\omega)^2/4S\hbar\omega$.

A complete analysis would also require that we consider the averaging over the different 'frozen' conformational states. A disentanglement of this effect to provide W as a function of the barrier

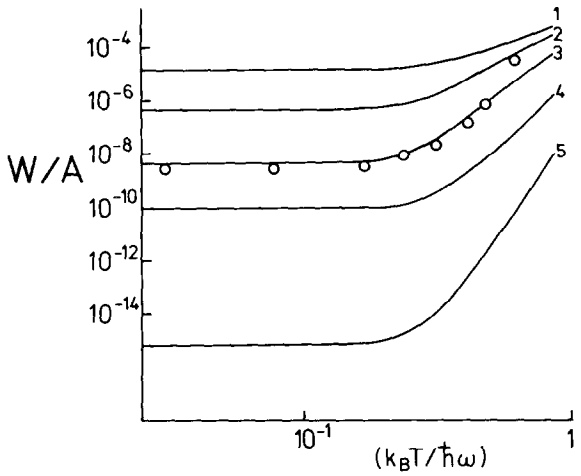

Fig.1. Model calculations of the nuclear Franck-Condon factors (W/A) ($A = 2\pi|V_{ab}|^2/\hbar^2\omega$) versus $k_BT/\hbar\omega$ for various values of S and p. The numbers correspond to the following parameters: (1) $S = 60, p = 30$; (2) $S = 30, p = 8$; (3) $S = 25, p = 2$; (4) $S = 80, p = 20$; (5) $S = 80, p = 20$. The circles show the experimental values [9] of log ($\tau_{0.75}^{-1}$) versus log T with the values at $T \to 0$ ($\tau_{0.75}^{-1} \to 5\ s^{-1}$ for $T \to 0$) matched with curve (3).

height without additional assumptions about the barrier geometry has in fact been given [9b,c]. However, since the distribution is relatively narrow around a peak barrier height, we shall take the rate constant as $\tau_{0.75}^{-1}$ and assume that it corresponds to fixed (peak) values of S and ΔE.

Figure 1 portrays plots of eq. (3) for various values of the parameters S and p. From a given value of ΔE (which is unknown for these processes) comparison of the high-temperature activation energy expression with the experimental value of this quantity (0.045 eV) gives $S\hbar\omega$. Moreover, the curves are all characterized by an activationless region up to $k_BT/\hbar\omega \simeq 0.1$–$0.2$ followed by a thermally activated region. Since the experimental plots display such a transition region at $T \simeq 10$–20 K this implies that $\hbar\omega \simeq 80$–$160\ cm^{-1}$, i.e., values which are not far from those expected for the metal–ligand bending modes of the heme complexes. Moreover, inspection of the plots reveals that $S = 20$–25 and $p = 2$–5 give the best fits which are also compatible with the high-temperature activation energy. This yields $\Delta E = -0.05$ eV for the energy gap and $E_r = 0.27$ eV for the reorganization energy. The value of S corresponds to a displacement of the Fe atom of 0.4–0.5 Å, in reasonable agreement with the available structural data [20–24]. Finally, we can utilize the low-temperature rate expression, eq. (4), together with the experimental low-temperature value of the rate constant $W(T \to 0) = 5\ s^{-1}$ and estimate V_{ab} to be 0.1–$1\ cm^{-1}$, which agrees well with our crude estimate of the second-order spin–orbit coupling matrix, eq. (2). Furthermore, this low value of V_{ab} justifies the nonadiabatic approach applied for the recombination dynamics of the CO/hb system.

We conclude that the general theory of nonadiabatic multiphonon electronic processes adopted to AT reactions provides a coherent description of the recombination reaction between CO and hemoglobin enabling us to sort out the electronic and the nuclear contribution to the dynamics of this interesting process.

References

[1] Devault, D. and Chance, B. (1966) Biophys. J. 6, 825–847.
[2] Dutton, P. L., Kaufmann, K. J., Chance, B. and Rentzepis, P. M. (1975) FEBS Lett. 60, 275–280.
[3] Peters, K., Avouris, P. and Rentzepis, P. M. (1978) Biophys. J. 23, 207–217.
[4] Chance, B., DeVault, D., Legallais, V., Mela, L. and Yonetani, T. (1967) in: Fast Reactions and Primary Processes in Chemical Kinetics (Claesson, S. ed) pp. 457–468, Interscience, New York.
[5] Blow, D. M. (1976) Acc. Chem. Res. 9, 145–152.
[6a] Wang, J. H. (1968) Science 161, 328–334;
[6b] Wang, J. H. (1970) Proc. Natl. Acad. Sci. USA 66, 874–881.
[7] Peters, K., Applebury, M. L. and Rentzepis, P. M. (1977) Proc. Natl. Acad. Sci. USA 74, 3119–3123.
[8] Bass, L. and Moore, W. J. (1973) Prog. Biophys. Mol. Biol. 27, 145–171.
[9a] Austin, R. H., Beeson, K. W., Eisenstein, L., Frauenfelder, H. and Gunsalus, I. C. (1975) Biochemistry 14, 5355–5373;
[9b] Alberding, N., Austin, R. H., Beeson, K. W., Chan, S. S., Eisenstein, L., Frauenfelder, H. and Nordlund, T. M. (1976) Science 192, 1002–1005;
[9c] Alberding, N., Chan, S. S., Eisenstein, L., Frauenfelder, H., Good, D., Gunsalus, I. C., Nordlund, T. M., Perutz, M. F., Reynolds, A. H. and Sorensen, L. B. (1979) Biochemistry, in press.
[10] Hopfield, J. J. (1974) Proc. Natl. Acad. Sci. USA 71, 3640–3644.
[11] Jortner, J. (1976) J. Chem. Phys. 64, 4860–4867.

[12] Kuznetsov, A. M., Sondergard, N. C. and Ulstrup, J. (1978) Chem. Phys. 29, 383–390.
[13] Dogonadze, R. R., Kharkats, Yu. I. and Ulstrup, J. (1973) J. Theor. Biol. 40, 259–277.
[14] Dogonadze, R. R., Kuznetsov, A. M. and Ulstrup, J. (1977) J. Theor. Biol. 69, 239–263.
[15] Marcus, R. A. (1956) J. Chem. Phys. 24, 966.
[16a] Levich, V. G. (1966) Adv. Electrochem. Electrochem. Eng. 4, 249.
[16b] Dogonaze, R. R. and Kuznetsov, A. M. (1973) Physical Chemistry. Kinetics, Viniti, Moscow.
[17] Kestner, N. R., Logan, J. and Jortner, J. (1974) J. Phys. Chem. 78, 2148–2166.
[18] Dogonadze, R. R., Kuznetsov, A. M. and Vorotyntsev, M. A. (1973) Dokl. Akad. Nauk SSSR, Ser. Fiz. Khim. 209, 1135–1138.
[19] Jortner, J. and Ulstrup, J. (1979) submitted.
[20] Bolton, W. and Perutz, M. F. (1970) Nature 228, 551–552.
[21] Perutz, M. F., Heidner, E. J., Ladner, J. E., Beetlestone, J. G., Ho, C. and Slade, E. F. (1974) Biochemistry 13, 2187–2200.
[22] Watson, H. C. (1968) Progr. Stereochem. 4, 299–333.
[23] Norvell, J. C., Nunes, A. C. and Schoenborn, B. P. (1975) Science 190, 568–571.
[24] Tanako, T. quoted in [31].
[25] Rifkind, J. M. (1973) in: Inorganic Biochemistry (Eichhorn, G. I. ed) vol. 2, pp. 832–891, Elsevier, Amsterdam.
[26] Peng, S.-M. and Ibers, J. A. (1976) J. Am. Chem. Soc. 98, 8032–8036.
[27a] Englman, R. and Jortner, J. (1970) Mol. Phys. 18, 145–164;
[27b] Freed, K. F. and Jortner, J. (1970) J. Chem. Phys. 52, 6272–6291;
[27c] Dogonadze, R. R., Kuznetsov, A. M. and Vorotyntsev, M. A. (1972) Phys. Stat. Sol. b 54, 125–134.
[28] Levich, V. G., Dogonadze, R. R., German, E. D., Kuznetsov, A. M. and Kharkats, Yu. I. (1970) Electrochim. Acta 15, 353–367.
[29] Holstein, T. (1978) Phil. Mag. 37, 499–526.
[30] Boucher, L. and Katz, J. J. (1967) J. Am. Chem. Soc. 69, 1340–1345.
[31] Olafson, B. D. and Goddard, W. A., iii (1977) Proc. Natl. Acad. Sci. USA 74, 1315–1319.